

# Feasibility Analysis of Subsea DC Distribution Grid for Oil Processing Projects

Tiago C.A. Soares, Antonio C. S. Lima and Sebastião E. M. Oliveira

**Abstract** – There is a need to develop new technologies allowing to explore reservoirs far away from the shore, with severe sea and/or weather conditions. The so-called Subsea processing which is basically a distribution system is a feasible solution as it can reduce significantly the number of offshore platforms.

This paper investigates the technical feasibility of a medium voltage offshore project using DC for both transmission and subsea distribution. The main components are presented, describing their models and showing simulations of some cases. The controls strategy of the rectifier and the inverters are also presented.

**Keywords:** power electronics, subsea systems, DC grid.

## I. INTRODUCTION

MANY oil operators are aiming to explore areas in the so-called new frontiers of oil, which consists the regions with difficult access due to surface weather conditions and great distance between the field and the coast [1]. The last condition is typical for the pre-salt oil fields in Brazil. Typically in this case, the oil companies are considering eliminating the offshore platforms, installing all of their equipment subsea, reducing operational costs and logistics problems [2]. Furthermore, several oil fields have been reaching maturity, decreasing the surge pressure and increasing the percentage of water in the oil recovered, bottlenecking the platforms, which were designed to process a lower quantity of water from the wells. Both situations result in lower profits. Such scenarios is leading the oil companies to invest in subsea processing and boosting, so they can increase the oil recovery rate in the fields and anticipate revenue [3]. However, this vision can become true only by developing adequate subsea processing, controls and power equipment [11]. As a consequence, there are several companies developing subsea power equipment, like transformers, variable speed drives (VSD), circuit breakers, connectors, to name just a few. Currently, there is a great movement toward developing subsea HVAC equipment, like transformers, switchgears, VSDs. For the transmission of higher power ratings, electric manufacturers are proposing to increase the voltage of the transmission and/or decrease drastically the

transmission frequency. The main purpose is to avoid compensating bulk reactive power [5], which becomes really difficult at subsea power grids, because it might be necessary to install additional subsea equipment, increasing the number of wet-mate connections (higher costs and lower reliability). There is also the question whether or not a DC system should be used in favor of conventional AC transmission. Typically, DC transmission is recommended only for very long distances [6]. However, the use of a subsea system may allow the reduction of the overall cost of the umbilical cable used for the power transmission [7]. The umbilical cable is the most expensive item of a subsea electrical grid. It comprises the power cables reinforced with mechanical structure to withstand dynamic and static loads. Such complex item has been used on point-to-point connections, with motors rated mainly between 4 and 6 kV. The low voltages are due to dimension restriction of the penetrators (responsible for the electrical feedthrough connections at the motors) of motors installed inside the wells. This very strict dimension restriction no longer exists when the motors are installed on the seabed, inside Modules of Boosting (MoBos), allowing the voltage increase of the transmission of point-to-point connections.

With the use of more MoBos close to each other, it is becoming impractical (excessive number of topside VSDs) and uneconomical the use of several point-to-point connections instead of a power grid sharing a single umbilical. As every motor needs to be controlled, the traditional solution being developed is to transmit the power through a shared umbilical using step-up and step-down transformers and to distribute through a bus bar and dedicated switchgears and VSDs. As each motor needs to be controlled by an inverter, it makes much more sense (technically and economically) to use a higher voltage at the output of the rectifier to transmit power using direct current in order to eliminate the need of transformers, decrease the losses and avoid issues related to an AC system.

In this paper we propose to use a subsea DC transmission and distribution even for small and medium scale projects based on existing technology. It is organized as follows: In the following section the configuration considered is detailed. The adaptation of the several equipment involved such as transformers, VSDs, motor for the subsea environment are not analyzed here since it can be considered a matter of engineering development rather than a technological challenge. In Section III, several test cases are presented to evaluate the system performance under disturbance and steady-state conditions. The main conclusions of this paper are presented in Section IV.

---

Paper submitted to the International Conference on Power Systems Transients (IPST2015) in Cavtat, Croatia June 15-18, 2015  
This work was partially financed by INERGE, CNPq, CAPES and FAPEMIG.  
The authors are with the Federal University of Rio de Janeiro, Rio de Janeiro, Brazil.

## II. SYSTEM DESCRIPTION

The proposed electrical grid is comprised mainly of a shared topside rectifier, umbilical cable and subsea DC bus bar and a dedicated DC circuit breaker and inverter to each motor. The circuit used in the simulation was modeled in the Simulink environment. Fig. 1 depicts the configuration considered. It is divided between topside, i.e. above sea level, and subsea equipment. The topside equipment are represented by a voltage source and a rectifier, responsible for the supply of a voltage controlled DC power to the subsea loads. Downstream the rectifier, a reactor and capacitor were used to damp voltage and current ripple. The subsea equipment are comprised of three sets of inverters and a permanent magnet motor. Every motor has a shaft power of approximately 1.05 MW. The topside and the subsea bus bar are connected through a 30 km umbilical cable. The losses at the bus bar and at the subsea electrical connectors were not considered. The models of the main components used in the simulations are described next.

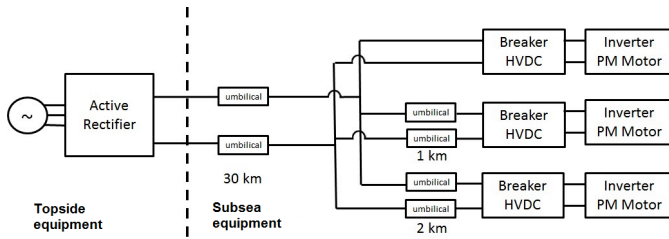


Fig. 1. Proposed electrical grid

### A. Rectifier

The rectifier considered here is based on an active one which is comprised by a rectifier bridge with six IGBT [4][5][8], which is responsible for the control of the voltage level at the umbilical. Upstream of the rectifier, there is a small reactor at each phase ( $L_{abc}$ ) and downstream of it, there are inductors and a capacitor to decrease the ripple at the umbilical. The input voltage from the source is 6.6 kV. For the control of the rectifier, three measurements are needed as shown in Fig. 2:

- Input voltage and current of the rectifier ( $V_{abc\ gen}$  and  $I_{abc\ gen}$ ).
- Output voltage of the rectifier ( $V_{dc\ meas}$ ).

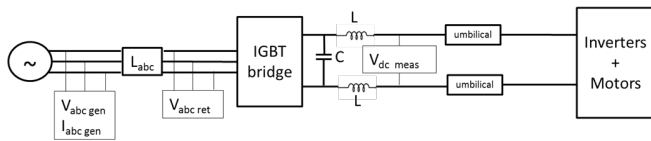


Fig. 2. Scheme of the components and measurements of the rectifier

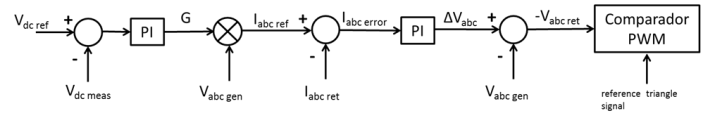


Fig. 3. Rectifier control block diagram.

The control is based on current control and its scheme is shown in Fig. 3. One advantages of this type of control is its robustness and simple implementation. The control is designed to align the phases of the input currents to the phases of phase-to-ground voltages, allowing a very high power factor, and their magnitude proportional to the load conductance, keeping the output voltage at 13.8 kV at steady state.

The rectifier output voltage is measured ( $V_{dc\ meas}$ ) and compared to a reference value ( $V_{dc\ ref}$ ). The difference is the input of a proportional-integral controller and its result is the load conductance (umbilical, subsea distribution and all subsea loads). The value of the conductance ( $G$ ) is multiplied by the three phase-to-ground voltages ( $V_{abc\ gen}$ ), which is used as the reference currents of the controller ( $I_{abc\ ref}$ ). Then, these reference currents are compared to the input currents ( $I_{abc\ ret}$ ) and the errors are the input of the second proportional-integral controller. The output of the controller gives the voltage drop at the input reactors, which are subtracted from the reactors' upstream phase-to-ground voltages and give the voltage references for the control of the IGBTs.

### B. Umbilical and DC distribution

The shared umbilical is responsible for the transmission of electrical power between topside and subsea equipment. Umbilicals with smaller cross sections were used between the bus bar and the inverters. In this paper, all the umbilical cables considered (transmission and distribution) were treated as frequency independent distributed parameters. We used manufacturer provided data. For the main umbilical, the one with 30 km length, a cable of 240 mm<sup>2</sup> was used. The cable parameters based on a single-phase equivalent at 60 Hz are: Resistance: 0,099 Ω/km; Inductance: 0,408 mH/km and Capacitance: 0,383 μF/km

For the umbilical cable used between the motor and the bus bar, a 120 mm<sup>2</sup> cable was considered. Its electrical parameters are, assuming 60 Hz: Resistance: 0.199 Ω/km; Inductance: 0.343 mH/km; Capacitance: 0.430 μF/km

### C. DC circuit breaker

Although the DC circuit breakers were developed according to [9], they are not considered in the simulations since the faults are cleared without the removal of any component from the grid as these scenarios are considered to be stricter for the control stabilization.

#### D. Inverters

Like the rectifier, the inverters are comprised of a bridge of six IGBTs with a capacitor upstream of it. Each inverter is responsible for the speed and torque control of the respective motor connected to it.

Vector control with PWM modulation was considered at the implementation of the inverter control [12]. Fig. 4 and Fig. 5 show the scheme of the control. Position sensor of the rotor and current measurement at the output of the inverter are needed for feedback.

The control is comprised of three closed loops: one to control the direct axis current, one to control the motor speed and another to control the quadrature axis current.

The first action of the controller is to measure the inverter output current and the rotor position of the motor in order to make the transformation of the currents to the dq axis, as described at (1), and to measure the speed of the motor.

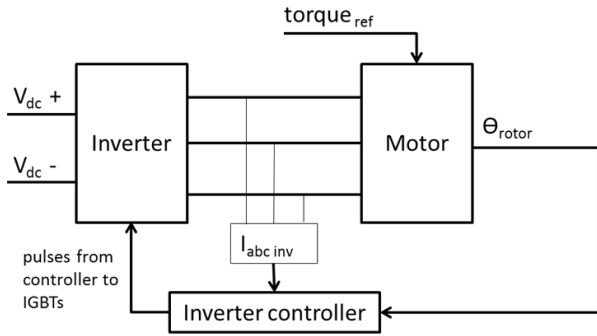


Fig. 4. Motor control scheme

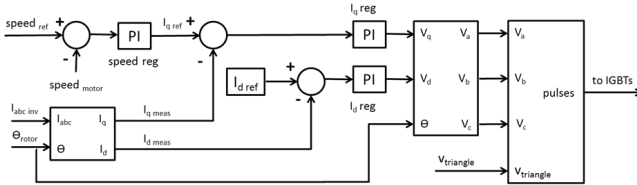


Fig. 5. Inverter control block diagram

The speed closed control compares the motor speed reference (speed<sub>ref</sub>) to the actual speed (speed<sub>motor</sub>) and the error passes through the proportional-integral controller, giving the input for the quadrature axis controller the current reference (I<sub>q ref</sub>). The quadrature axis current is responsible for the electromagnetic torque that lead the motor speed and the shaft torque to the specified values.

$$\begin{bmatrix} i_d \\ i_q \end{bmatrix} = \frac{2}{3} \times \begin{bmatrix} \cos \theta & \cos\left(\theta - \frac{2\pi}{3}\right) & \cos\left(\theta - \frac{4\pi}{3}\right) \\ -\sin \theta & -\sin\left(\theta - \frac{2\pi}{3}\right) & -\sin\left(\theta - \frac{4\pi}{3}\right) \end{bmatrix} \begin{bmatrix} i_a \\ i_b \\ i_c \end{bmatrix} \quad (1)$$

Then, the quadrature axis reference current is compared to the measured one (I<sub>q meas</sub>). The measure direct axis current (I<sub>d meas</sub>) is also compared to the reference value (equal to zero).

Both current errors are again the input for two distinct proportional-integral controllers and the outputs are the reference V<sub>d</sub> and V<sub>q</sub> voltages. After an inverse transformation

as per (2), the phase-to-ground reference voltages are found and used for the PWM modulation.

$$\begin{bmatrix} v_a \\ v_b \\ v_c \end{bmatrix} = \begin{bmatrix} \cos \theta & -\sin \theta \\ \cos\left(\theta - \frac{2\pi}{3}\right) & -\sin\left(\theta - \frac{2\pi}{3}\right) \\ \cos\left(\theta - \frac{4\pi}{3}\right) & -\sin\left(\theta - \frac{4\pi}{3}\right) \end{bmatrix} \begin{bmatrix} v_d \\ v_q \end{bmatrix} \quad (2)$$

#### E. Motors

The motors considered at the simulations are permanent magnet motors (PMM), which can be considered more efficient than induction motors, reducing the power transmitted through the umbilical.

Other advantages of PMM are that they are more compact, due to higher power density, can reach higher speeds (more operational flexibility) and lower control of water contamination in the dielectric fluid in the gap is needed.

The motor used in the simulations are 2-pole, with rounded rotor. The shaft power is 1.05 MW, the speed is 4000 rpm and the terminal voltage is 6 kV.

### III. SIMULATION RESULTS

#### A. Steady state

The first case to be analyzed is the system behavior during the acceleration of three motors to 4000 rpm simultaneously with a constant shaft torque of 2500 N.m. Prior the start of the simulation, all the components of the system are de-energized and the motors are stopped. Right after the energization of the system through the rectifier, a current of up to 1100 A was measured at the umbilical, making the control to react, causing an overvoltage of 20 %. Considering a margin of 5 % around the voltage set point for the stabilization, the system can be considered stabilized approximately 0.2 s after the start of the simulation.

The motors accelerated and reached the steady state speed at 0.5 s, when the motors dynamics caused some disturbances at the system, corrected in less than 0.1 s. Therefore, the system can be considered stabilized again at instant 0.6 s. The voltage drop across the umbilical is 12 %, considered acceptable for such projects. The power factor of the rectifier was 0.964. Fig. 6 and 7 show the voltage and current behavior at the output of the rectifier during system start up.

#### B. Phase-to-ground fault at phase A of the motor closer to the bus bar

In this situation, a fault at phase A at the terminal of the motor closer to the bus bar was simulated. The fault occurred after the system is in steady state. The duration of the fault was 0.15 s through a 0.1 Ω resistance between phase A and the ground [10].

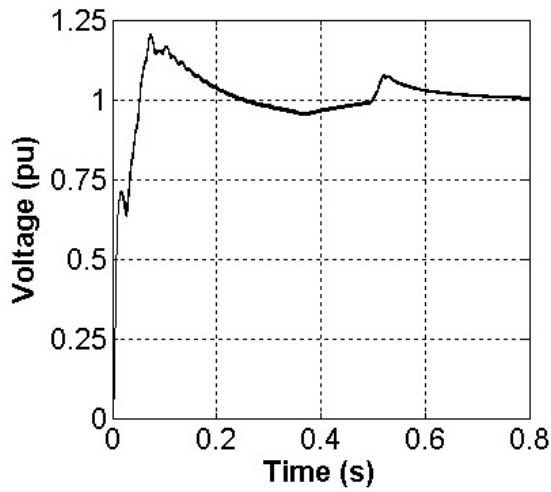


Fig. 6. Rectifier output voltage

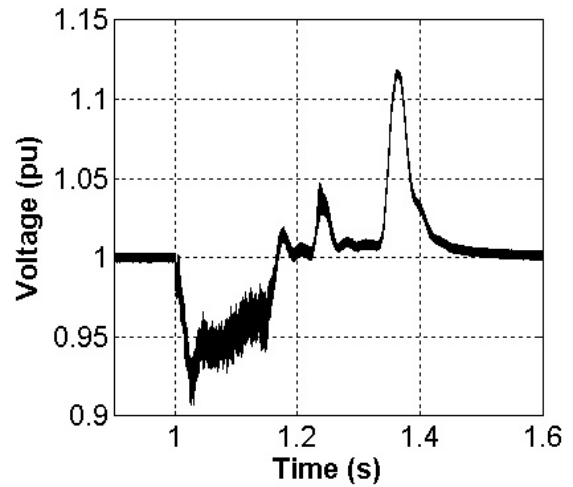


Fig. 8. Rectifier output voltage

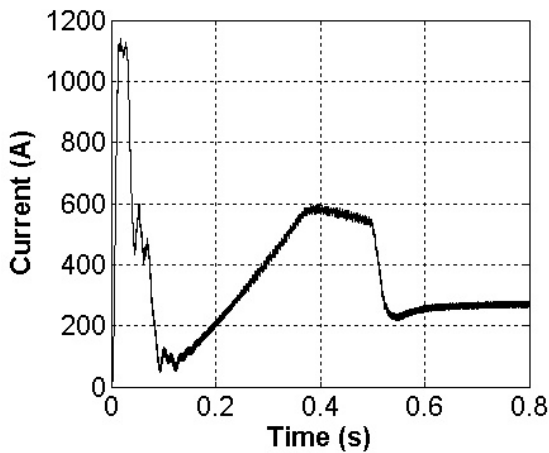


Fig. 7. Rectifier output current

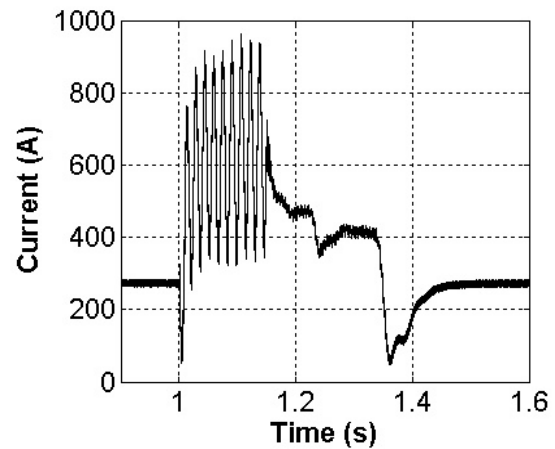


Fig. 9. Rectifier output current.

In the instant of the fault the current at the output of the rectifier becomes very oscillatory and starts increasing until 950 A while the voltage drops almost to 0.9 pu (Fig. 8 and 9). At the point of the fault, the current increases to 4500 A and the voltage on phases B and C increase from 6000 V to 9500 V (Fig. 10 and 11).

At the adjacent motor's terminals (Fig. 12), connected to the common bus bar by one kilometer of 120 mm<sup>2</sup> cable, the current decreased 50 %, but there was a relevant overvoltage (30 kV at phases A and B and 45 kV at phase C).

After the fault, the system recovers the stability instantly, but because of the motors, the system suffers more two disturbances at instants 1.23 s (due to the motor closer to the bus bar) and 1.33 s (due to the other two motors). The former disturbance causes at the output of the rectifier an overvoltage of 5 % (still stable) and the latter 13 %. After the last disturbance, the system stabilizes again after 0.05 s.

The system is totally stabilized at instant 1.38 s, 0.23 s after the removal of the fault.

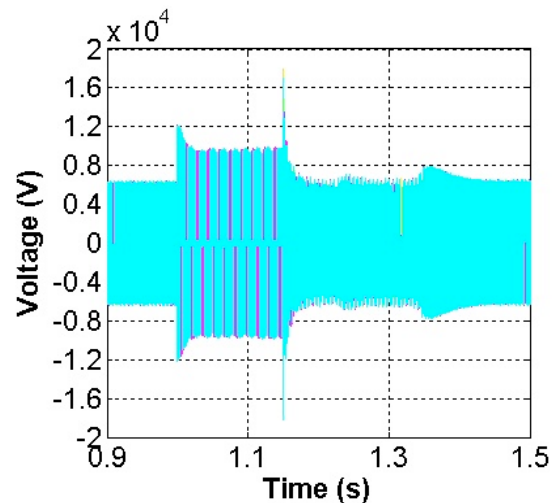


Fig. 10. Voltage at the terminal of the motor where the fault occurred.

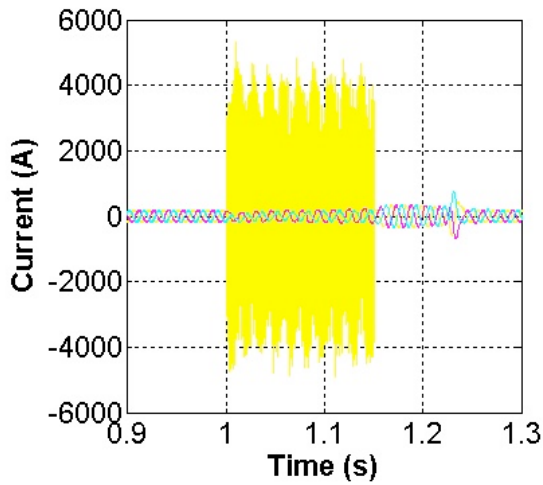


Fig. 11. Current at the terminal of the motor where the fault occurred.

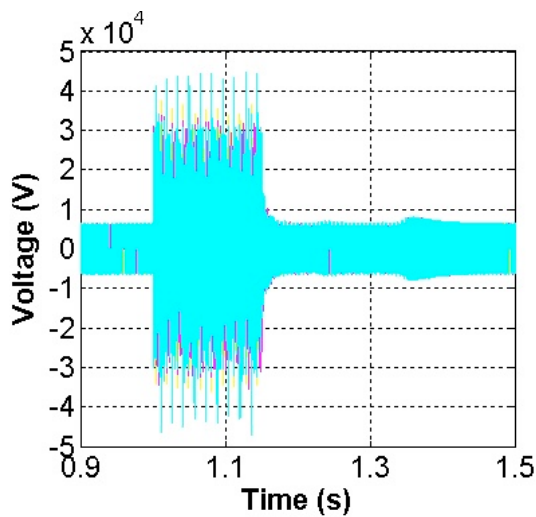


Fig. 12. Voltage at the terminal of the motor 1 km away from the fault.

### C. Phase-to-ground fault at phase A of the rectifier

The last case to be discussed is a phase-to-ground fault with the same conditions of the second case, but in the phase A of the rectifier. As can be seen on Figs. 13 to 16, this fault caused little disturbance on the output voltage of the rectifier. The output current becomes very oscillatory and increases, affecting the motors terminal voltages. The inverter output current and the motors' torque and speed disturbances can be considered negligible. After the removal of the fault, the system returns to steady state immediately.

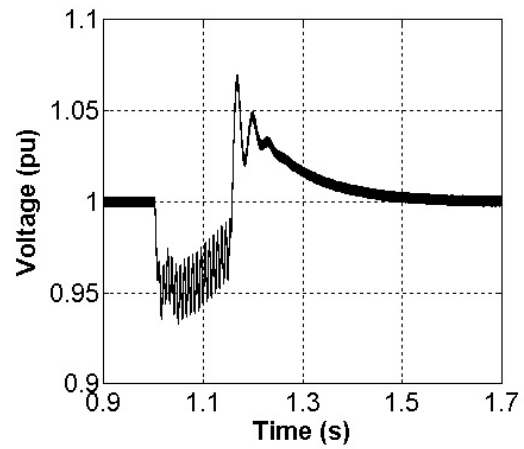


Fig. 13. Rectifier output voltage.

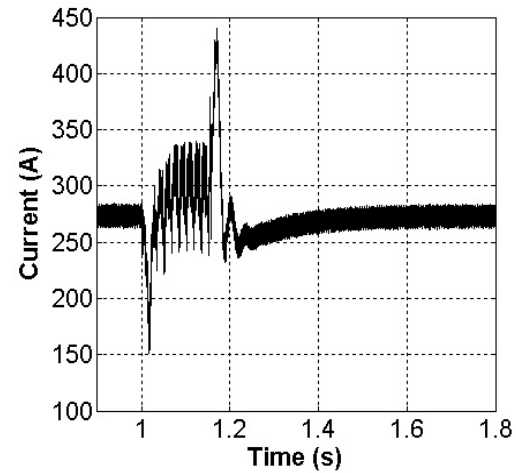


Fig. 14. Rectifier output current.

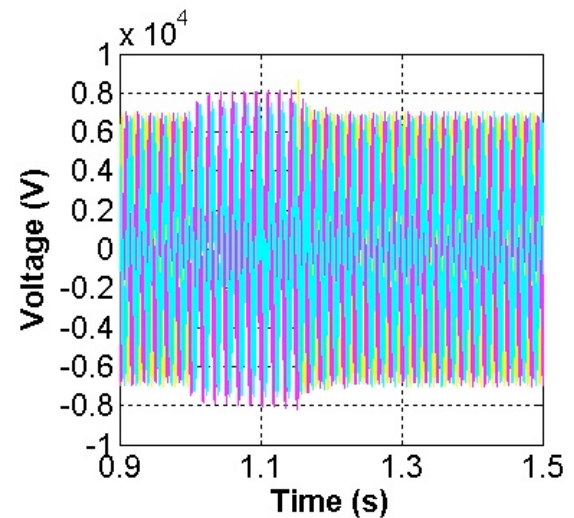


Fig. 15. Rectifier input voltage (fault point)

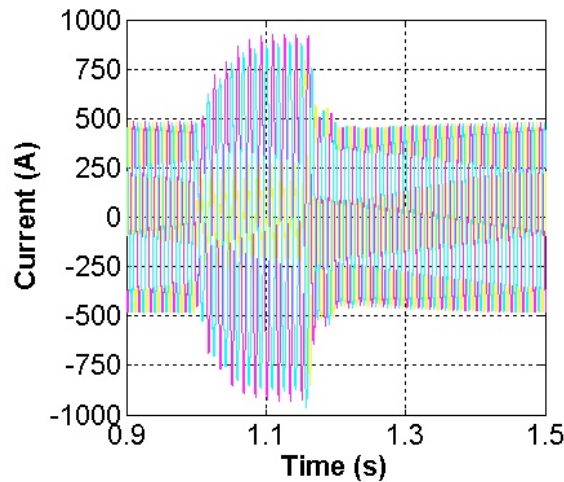


Fig. 16. Rectifier input current (fault point)

#### IV. CONCLUSIONS

This paper proposes an electrical grid topology feasible for subsea processing projects. It is comprised of both DC transmission and distribution with components of low technologic risk. The simulation results showed that the system is simple and robust, capable of withstanding the most common faults that can occur at the system by stabilizing it as soon as the fault is removed.

DC transmission is currently only being considered for long step-out transmission of bulk power. This conservative approach may bring higher costs and challenges for future subsea processing projects, but can be avoided if DC transmission and distribution be considered for a larger range of projects.

Future work will deal with the improvement of the models involved and the establishment of control and monitoring techniques capable of maintaining the system reliability.

#### REFERENCES

- [1] TOTAL. "EOR maximizing recovery factors". 2009. [Online]. Available: [http://www.geoscopie.fr/images/upload/geoscopie/espace\\_pedagogique/total-eorbis-gb2.pdf](http://www.geoscopie.fr/images/upload/geoscopie/espace_pedagogique/total-eorbis-gb2.pdf)
- [2] O. Okland, S. Davies, R. M. Ramberg and H. Rogno. "Steps to the Subsea Factory", *OTC 24307*, Rio de Janeiro, 2013.
- [3] Knowledge Reservoir, "MMS Enhanced Recovery Study". 2010. [Online] Available: [http://www.bsee.gov/uploadedfiles/bsee/research\\_and\\_training/technology\\_assessment\\_and\\_research/665aa.pdf](http://www.bsee.gov/uploadedfiles/bsee/research_and_training/technology_assessment_and_research/665aa.pdf)
- [4] C. Chen, C. Lee, R. Tu, and G. Horng. "A Novel Simplified Space-Vector-Modulated Control Scheme for Three-Phase Switch-Mode Rectifier", *IEEE Transactions on industrial electronics*, vol. 46, n. 3, pp. 512–516, 1999.
- [5] G. Asplund, K. Eriksson, H. Jiang, J. Lindberg, R. Pålsson and K. Svensson. "DC Transmission Based On Voltage Source Converters", *CIGRÉ SC14 Colloquium*, South Africa, 1997.
- [6] S. J. Shao and V. G. Agelidis, "Review of DC System Technologies for Large Scale Integration of Wind Energy Systems with Electricity Grids", *Energies*, n. 3, ISSN 1996-1073, pp. 1303–1319, 2010.
- [7] A. Mæland and R. S. Chokhawala, "Powering Oil & Gas Offshore Operations from Mainland Electrical Grid", *World Energy Congress*, Montreal, 2010.
- [8] F. Wang, L. Bertling, T. Le, A. Mannikoff and A. Bergman. "An Overview Introduction of VSC-HVDC: State-of-art and Potential Applications in Electric Power Systems", *CIGRÉ Session*, Bologna, 2011
- [9] M. Callavik, A. Blomberg, J. Häfner and B. Jacobson. "The Hybrid HVDC Breaker, An innovation breakthrough enabling reliable HVDC grids", *ABB Grid Systems Technical Paper*, 2012.
- [10] M. O. Faruque, Y. Zhang and V. Dinavahi, "Detailed Modeling of CIGRÉ HVDC Benchmark System Using PSCAD/EMTDC and PSB/SIMULINK", *IEEE Transactions On Power Delivery*, v. 21, n. 1, pp. 378–387, 2006.
- [11] E. Baggerud, V. Sten-Halvorsen, R. Fantoft, "Technical Status and Development for Subsea Gas Compression", *Offshore Technology Conference 18952*, Houston, 2007.
- [12] PED4-1038C, "Torque Control in Field Weakening Mode". M.Sc. dissertation, Aalborg University, Copenhagen, 2009.